

Hiding its age: the case for a younger bulge

M. Haywood¹, P. Di Matteo¹, O. Snaith², A. Calamida³

¹ GEPI, Observatoire de Paris, CNRS, Université Paris Diderot, 5 place Jules Janssen, 92190 Meudon, France
e-mail: Misha.Haywood@obspm.fr

² School of Physics, Korea Institute for Advanced Study, 85 Hoegiro, Dongdaemun-gu, Seoul 02455, Republic of Korea

³ National Optical Astronomy Observatory/AURA, Tucson, AZ 85719

Accepted, Received

ABSTRACT

The determination of the age of the bulge has led to two contradictory results. On the one side, the color-magnitude diagrams in different bulge fields seem to indicate a uniformly old (>10 Gyr) population. On the other side, individual ages derived from dwarfs observed through microlensing events seem to indicate a large spread, from ~ 2 to ~ 13 Gyr. Because the bulge is now recognised as being mainly a boxy peanut-shaped bar, it is suggested that disk stars are one of its main constituents, and therefore also stars with ages significantly younger than 10 Gyr. Other arguments as well point to the fact that the bulge cannot be exclusively old, and in particular cannot be a burst population, as it is usually expected if the bulge was the fossil remnant of a merger phase in the early Galaxy. In the present study, we show that given the range of metallicities observed in the bulge, a uniformly old population would be reflected into a significant spread in color at the turn-off which is not observed. Inversely, we demonstrate that the correlation between age and metallicity expected to hold for the inner disk would conspire to form a color-magnitude diagram with a remarkably small spread in color, thus mimicking the color-magnitude diagram of a uniformly old population. If stars younger than 10 Gyr are part of the bulge, as must be the case if the bulge has been mainly formed through dynamical instabilities in the disk, then a very small spread at the turn-off is expected, as seen in the observations.

Key words. Galaxy: abundances — Galaxy: disk — Galaxy: evolution — galaxies: evolution

1. Introduction

Progress in the study of galactic bulges in the last decade have established that they come in two different flavours: classical and pseudo-bulges (Kormendy & Kennicutt 2004). Classical bulges have properties identical to elliptical galaxies, while pseudo-bulges have properties inherited from the disk from which they are supposedly formed: they are more flattened, have bluer colors, and rotate faster. In the local volume (distance < 11 Mpc), pseudo-bulges are the majority, and classical bulges are few (Kormendy et al. 2010; Fisher & Drory 2010), while some galaxies are known to harbour the two types of bulges (Erwin et al. 2015; Fisher & Drory 2016). It has been found first from kinematic constraints that the classical bulge must be small or inexistent (Shen et al. 2010; Kunder et al. 2012; Di Matteo et al. 2014) in the Milky Way (hereafter MW). At the same time, arguments based on kinematic and chemical properties of stellar populations observed in the bulge of the MW have strengthen the picture of a pseudo-bulge with clear correspondence between the stellar populations identified in the bulge and those of the inner disk of the Galaxy. Hence, in the nomenclature of Ness et al. (2013), it has been suggested that components A, B and C could be identified to the thin disk, young and old thick disk of the MW (Di Matteo et al. 2014, Di Matteo 2016). The expectations, based on the recognition that the bulge of the MW is a pseudo-bulge, together with the chemical arguments, are therefore that most of the bulge have a disk origin, implying that it should contains stars of all ages (Ness et al. 2013).

Clarkson et al. (2008) (hereafter CL08) selected a pure sample of bulge stars in the Sagittarius Window Eclipsing Extrasolar Planet Search (SWEPS) field by using proper motion measurements based on Hubble Space Telescope data. They obtained the color-magnitude diagram (CMD) which is to date the strongest support for an old bulge, showing a tight old turn-off and no significant upper main sequence. The very tight CMD in the region of the turn-off has been confirmed in Calamida et al., (2015, hereafter CA15). Bensby et al. (2011, 2013) have measured metallicities and abundances of microlensed dwarfs stars in the bulge, estimating their age. They found that the bulge shows a large spread in age, with stellar ages ranging from less than 3 up to 13 Gyr. While Clarkson et al. (2011) estimate that not more than 3.5% of bulge stars may have an age smaller than 5 Gyr, this percentage rises to 22% for the microlensed dwarfs studied by Bensby et al., (2013, hereafter B13). Clearly, stars younger than about 10 Gyr are a significant fraction of the bulge according to the results of B13. The present picture is therefore contradictory, and the arguments seem to be incompatible (see also Nataf 2015).

In their study, B13 suggest that a correlation between age and metallicity could conspire to produce stars which would be located in a relatively narrow sequence in the HR diagram, giving the impression of a co-eval, old population, as observed by CL08. This idea has received little attention however, possibly because one may think that such 'conspiracy' would require a very specific, and ad-hoc bulge chemical evolution. In the present study, we first show that

an exclusively old bulge, combined with the large spread in metallicity that is observed in the bulge, cannot produce the tight turn-off observed in the HST CMD. We then show that if the metal-rich stars are younger, the disagreement is considerably reduced, and obtaining a dispersion compatible with the one observed is becoming possible. The problem is not that the apparently old bulge turn-off is incompatible with significantly young stars, but to understand how and how much young stars can hide in the bulge CMD.

The outline of the present article is as follows. We first introduce our chemical evolution model of the inner disk and the age-metallicity relation (hereafter AMR) obtained from this model. A detailed comparison with the observed properties of the inner disk and the bulge can be found in Haywood et al. (in preparation). We then give a brief description of the properties of the SWEEPS's Window (CL08) and the constraints from the SWEEPS CMDs. In Section 3 we explain how we reconstruct the CMD of the bulge when assuming the AMR of our model or a co-eval population. In the third section, we present realistic simulations of the CMD of the bulge which are discussed in the light of the known characteristics of the observed CMDs. In the last section, we discuss our results in the context of the bulge evolution and review the other arguments that have been invoked to claim that the bulge is exclusively old.

2. The chemical evolution model and observational constraints

We aim at understanding under which conditions on the age distribution of stars the CMD of the bulge, and particularly the CMD obtained by CL08 or CA15 can be reproduced. To first order, the density of stars in a color-magnitude diagram results from its star formation history (masses and ages) and correlated chemical evolution (metallicities and abundances). This can standardly be represented by an initial mass function (IMF), a star formation history (SFH), and the variation of metallicity and element abundances with age. We therefore need to adopt a model which describes these evolutions.

2.1. Chemical evolution model

In Snaith et al. (2015) we described a model which was fitted to the thick and thin disk data of stars at the solar vicinity. A SFH of the inner disks was derived by fitting the model to the age-[Si/Fe] relation found in Haywood et al. (2013) on solar vicinity stars. In Haywood et al. (2015), we showed that this age-[Si/Fe] relation is a general property of the inner disk, implying that the SFH of Snaith et al. (2015) is also valid for the whole inner disk. In Haywood et al. (2016), we showed further that our model provides a very good match to the inner disk APOGEE abundance data. Improvements in the observations of the bulge in the last ten years have shown that the alpha elements, while originally believed to be significantly higher than those of the solar vicinity (see e.g. Lecureur et al. 2007) are now measured to be near (Gonzalez et al. 2015), or similar (B13) to solar abundances, adding strong support to the idea that chemical evolution models could fit the bulge and disk chemical properties at the same time. In an accompanying study (Haywood et al. in preparation), we show

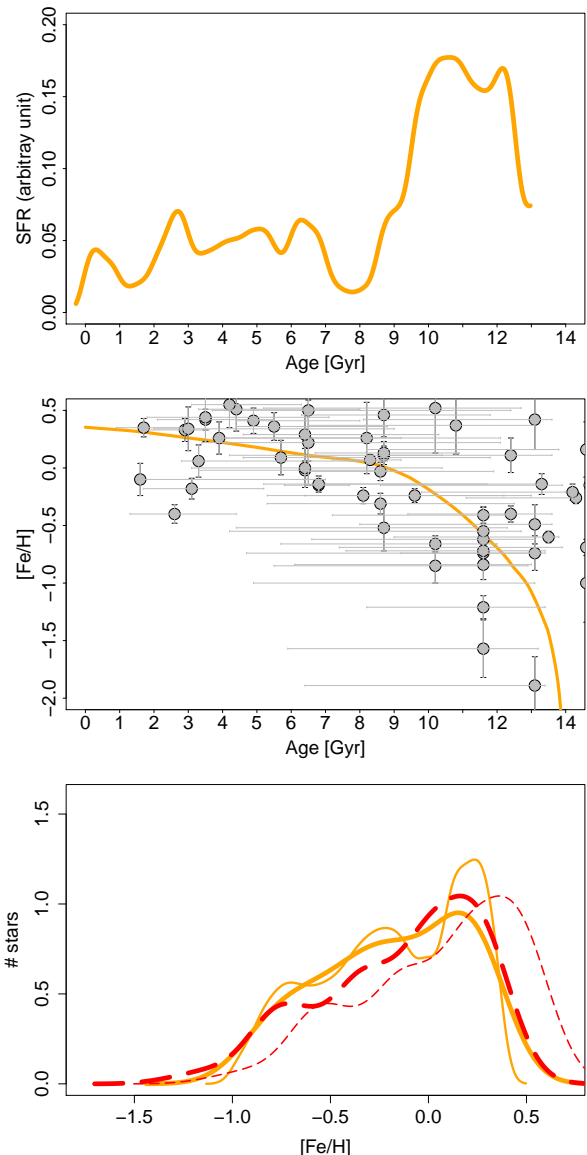


Fig. 1: Top: Star formation rate history of the model. Middle: age-metallicity relation of the model, together with the stellar age and metallicities of the microlensing events of bulge stars from B13. Bottom: the metallicity distribution from the model (thin orange curve) and convolved with a gaussian of 0.15 dex dispersion (thick orange curve) together with the generalised histograms of the observed MDF in the Baade's Window from Hill et al. (2011) (thin dashed red curve), and shifted by -0.21 dex (thick dashed red curve), following the results of Rojas-Arriagada et al. (2014).

indeed that the chemical properties of the bulge (chemical abundance patterns and metallicity distribution) are compatible with those to the inner thin disk and the thick disk of the MW, and that these properties can be well described by the same model which we used to represent the chemical evolution of inner disk stars. In a scenario where most of

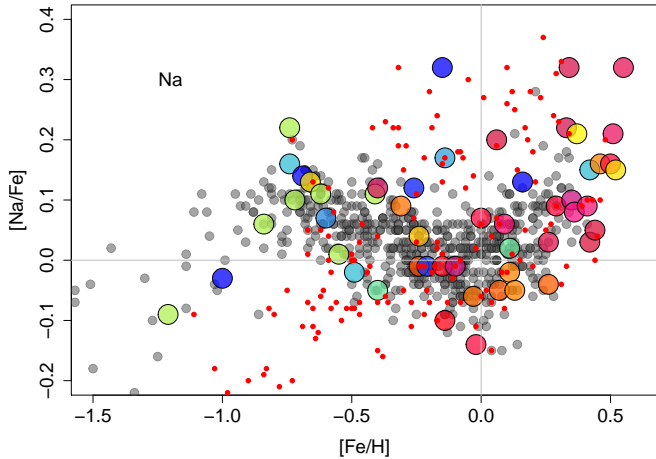


Fig. 2: Sodium abundance ratio as a function of $[\text{Fe}/\text{H}]$ for stars in the disk (gray dots) from Bensby et al. (2014) and for stars in the bulge (larger symbols) from B13. The data from Johnson et al. (2014) are shown as red dots.

the bulge forms by dynamical instabilities in the disk and its stars originate in the thick disk and inner thin disk, this is expected, and justifies that we use the age-metallicity relation and the SFH of our model as input parameters in building the CMDs of the bulge.

The ingredients of the model are described and discussed in detail in Snaith et al. (2015). These ingredients are: standard theoretical yields (Iwamoto et al. 1999; Nomoto et al. 2006; Karakas 2010), an IMF (Kroupa 2001) independent of time, and a stellar mass–lifetime relation dependent on the metallicity (Raiteri et al. 1996). The Kroupa (2001) IMF is in good agreement with the IMF estimated for the bulge in CA15. No instantaneous recycling approximation has been implemented, see Snaith et al. (2015) for details.

Fig. 1 shows the main distributions of the model resulting from fitting the age– $[\text{Si}/\text{Fe}]$ relation: the star formation history (a), age–metallicity relation (b) and metallicity distribution function (c). Fig. 1(b) compares the age–metallicity relation of the model with the data on microlensing events from B13. The MDF of the model (thin and thick continuous curves) is compared to the observed MDF from Hill et al. (2011, dashed thin curve, Fig. 1(c)) in the Baade’s Window. A systematic shift is apparent between the model and observed MDFs, of about 0.2 dex. More recently, Rojas-Arriagada et al. (2014) compared the metallicities of about 100 stars they have in common with Hill et al. (2011), and find an offset of 0.21 dex. The thick dashed red curve shows the Hill et al. (2011) MDF corrected by this amount. The observed MDF now shows good agreement with the model. The thick continuous curve shows the model convolved with a gaussian of 0.15 dex dispersion in order to take into account the measurement errors of observed metallicities. A detailed discussion on the comparison between abundances of the bulge and disk stars is beyond the present paper and is provided in Haywood et al. (2016). We comment however on the particular abundance of sodium, which is presented as the best evidence of a different chemical histories of the bulge and disk, on

the basis of the study of Johnson et al. (2014). Fig. 2 shows the abundance data of dwarfs in the solar vicinity from Bensby et al. (2014, grey dots), microlensed dwarfs of B13 and giants from Johnson et al. (2014). The figure illustrates that while dwarf data of the bulge and solar vicinity show good agreement, the bulge giants of Johnson et al. (2014) and bulge dwarfs of B13 (red and gray dots respectively) have very different distributions. Because the data of B13 and Bensby et al. (2014) are both obtained on dwarfs (and measured from the same authors), they are less prone to possible systematics. This plot illustrates that Na abundances of the bulge can be affected by significant uncertainties and the difference seen by Johnson et al. (2014) by comparing giants of the bulge and disk dwarfs of the solar vicinity may only be the effect of residual either between giants and dwarfs or in reduction procedures. We therefore conclude that sodium abundances of Johnson et al. (2014) provides no conclusive evidence of a real difference between the disk and bulge nucleosynthesis history, while the other two datasets of the bulge and disk dwarfs show excellent agreement.

The SFH, age–metallicity relation and MDF distributions of Fig. 1 are used to generate the CMDs discussed in Sec. 3.

2.2. The Galactic bulge SWEEPS field

In the bulge, spatial segregation occurs, with the most metal-poor (presumably older) populations dominating at larger distances from the Galactic plane, while in-plane fields are dominated by the most-metal-rich (presumably the youngest) component (Ness et al. 2013). The field observed by CL08, Clarkson et al. (2011) and CA15 at $l=1.25^\circ$ and $b=-2.65^\circ$ is 340pc below the Galactic plane at the distance of the bulge (8kpc). Hence, although the field is above the star formation layer, it may contain a significant number of stars a few Gyr old. However, young stars, if present, should be visible above the turn-off in the SWEEPS field, but no significant number have been detected (see CL08). Therefore, in the case where we consider that the bulge may have a significant spread in age, we assume that stars are 3 Gyr old or older.

In comparing with the data, a key ingredient is the metallicity distribution function. The MDF of the bulge is known to be a strong function of Galactic latitude (e.g. Ness et al. 2013), with the metal-rich component contribution decreasing at increasing latitude, but the spread in metallicity is large anywhere (Ness et al. 2013; Gonzalez et al. 2015).

According to Ness et al. (2013), the contribution of the metal-rich component (roughly $[\text{Fe}/\text{H}]>0.0$ dex, their component A) is already as important as the medium metal-poor component (component B in Ness et al. 2013) at $b=-5^\circ$. In Baade’s Window, the contribution of the metal-rich component is dominant (see e.g. Gonzalez et al. 2015), with a strong peak at $[\text{Fe}/\text{H}]\sim+0.25$ dex, very similar to the model distribution of Fig. 1, and a spread from $[\text{Fe}/\text{H}]=-1$ to 0.7 dex. Metallicities measured from medium-resolution spectroscopy in the SWEEPS field for 93 stars show a similar spread from -1 to 0.8 dex, also compatible with other previous studies (Hill et al. 2011; B13; Ness et al. 2013, see Calamida et al. 2014 for more details). Our model MDF reproduces fairly well these main features: a large spread in metallicity, and a prominent peak at super-solar

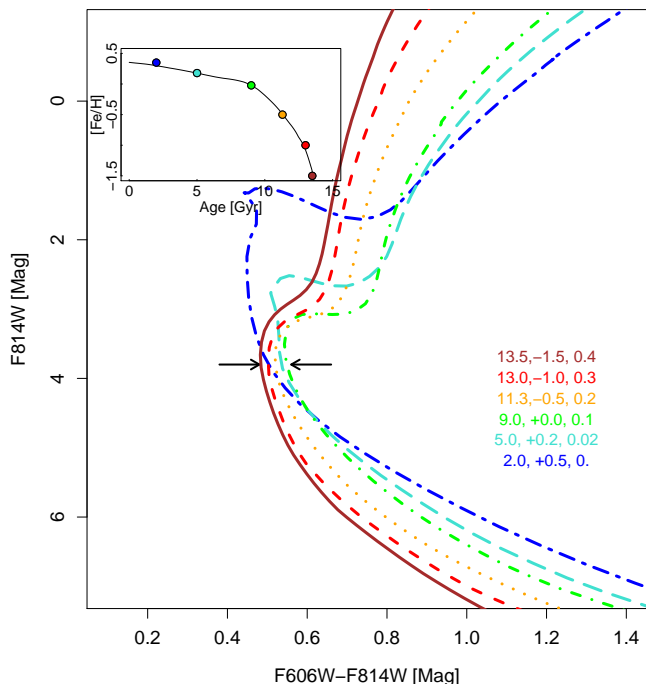


Fig. 3: Case (a): isochrones along the AMR of Fig. 1, also inset for ages 5, 7, 9, 10 and 13 Gyr. Corresponding metallicities and alpha abundances are given on the plot. The two arrows at the turn-off are separated by 0.07 mag. The age, metallicity and $[\alpha/\text{Fe}]$ abundance are given for each isochrone.

metallicities, or $[\text{Fe}/\text{H}] \sim +0.20$ dex. Metallicities below -1.0 dex represent 5% of the total in the model MDF, while observed MDF often have a negligible amount of stars below this limit. For a part, this may be due to the small statistics of most surveys (a few hundred stars). In Ness et al. (2013), where the number of objects is more than one order of magnitude higher than in other surveys, the tail at $[\text{Fe}/\text{H}] < -1.0$ dex is clearly visible, weighting about $1 \pm 1\%$ at $b = -5^\circ$ (Ness et al. 2013). In the following, we adopt the MDF of our model as a realistic representation of the MDF of the bulge in the Baade's Window or nearby SWEPS fields, but also evaluated the photometric dispersion at the turn-off when discarding stars with $[\text{Fe}/\text{H}] < -1.0$ dex.

In the CMD of CA15 (Fig. 4), the dispersion at the turn-off is 0.031 mag, and the spread, which we take as three standard deviations, is 0.093 mag¹. The contribution of the photometric and data deduction technique to the spread is estimated to be 0.028 mag. Deducing this contribution of the observed dispersion, we obtain a dispersion of 0.0295 mag. This dispersion is due to age, metallicity, contribution of binaries, differential extinction, and spread in distances of the stars. The intrinsic (due only to age and metallicity effects) dispersion at the turn-off is therefore extremely small and lower than 0.03 mag. We now seek

¹ In the remaining of the article, the term 'dispersion' is used for standard deviation, while the 'spread' is assumed as being 3 times the dispersion, and is taken as representative of the observed spread at the turn-off.

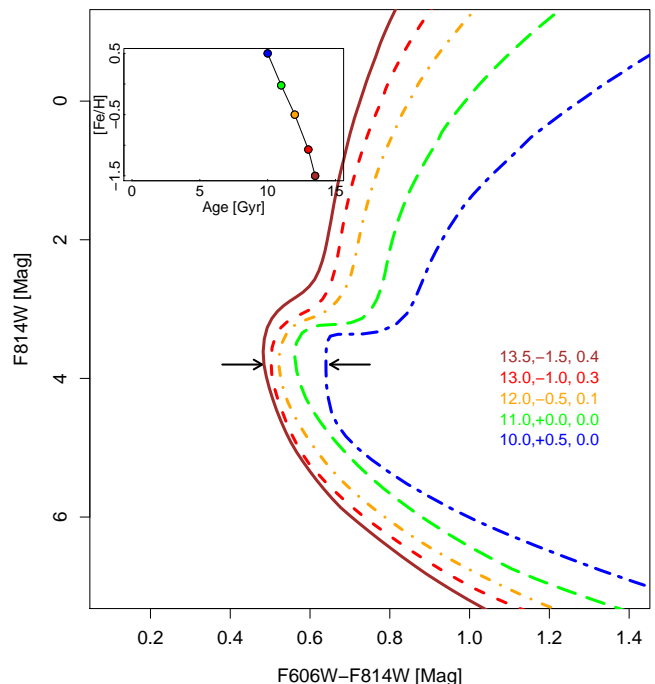


Fig. 4: Case (b): isochrones at 10, 11, 12, 13 and 13.5 Gyr and metallicities +0.3, 0.0, -0.5, -1.0 and -1.5 dex. The level of alpha elements is given on the plot. The two arrows at the turn-off are separated by 0.17 mag. The age, metallicity and $[\alpha/\text{Fe}]$ abundance are given for each isochrone.

to understand at what condition on age a synthetic CMD is compatible with such a narrow turn-off given the very wide distribution of metallicities observed in the bulge, and taking into account all the effects just mentioned through Monte-Carlo simulations.

3. The color-magnitude diagram of the Bulge

We have built CMDs considering three different cases. In case (a) the AMR is represented by our model. In case (b), the bulge is considered exclusively old (>10 Gyr), but a relation still links age to metallicity, while in case (c), we considered that stars are born in a burst and all have an age of 11 Gyr.

3.1. Isochrones

Fig. 3 (case a) shows a set of isochrones in the (F814W, F606W-F814W) plane, covering the age range from 2 to 13.5 Gyr. Their metallicity is chosen according to the AMR from our model and represented in the inset frame. The isochrones are calculated at the metallicity and alpha abundance content shown on each plot from the Yale library (Demarque et al. 2004). The conversion to the ACS-WFC F814W, F606W bands uses colors from the Dartmouth database (Dotter et al. 2008), which are based on the work of Bedin et al. (2005). On Fig. 3, although the age spanned by the isochrones is 11.5 Gyr (2 to 13.5 Gyr), the range in color at the turn-off of the old populations (F606W-F814W)

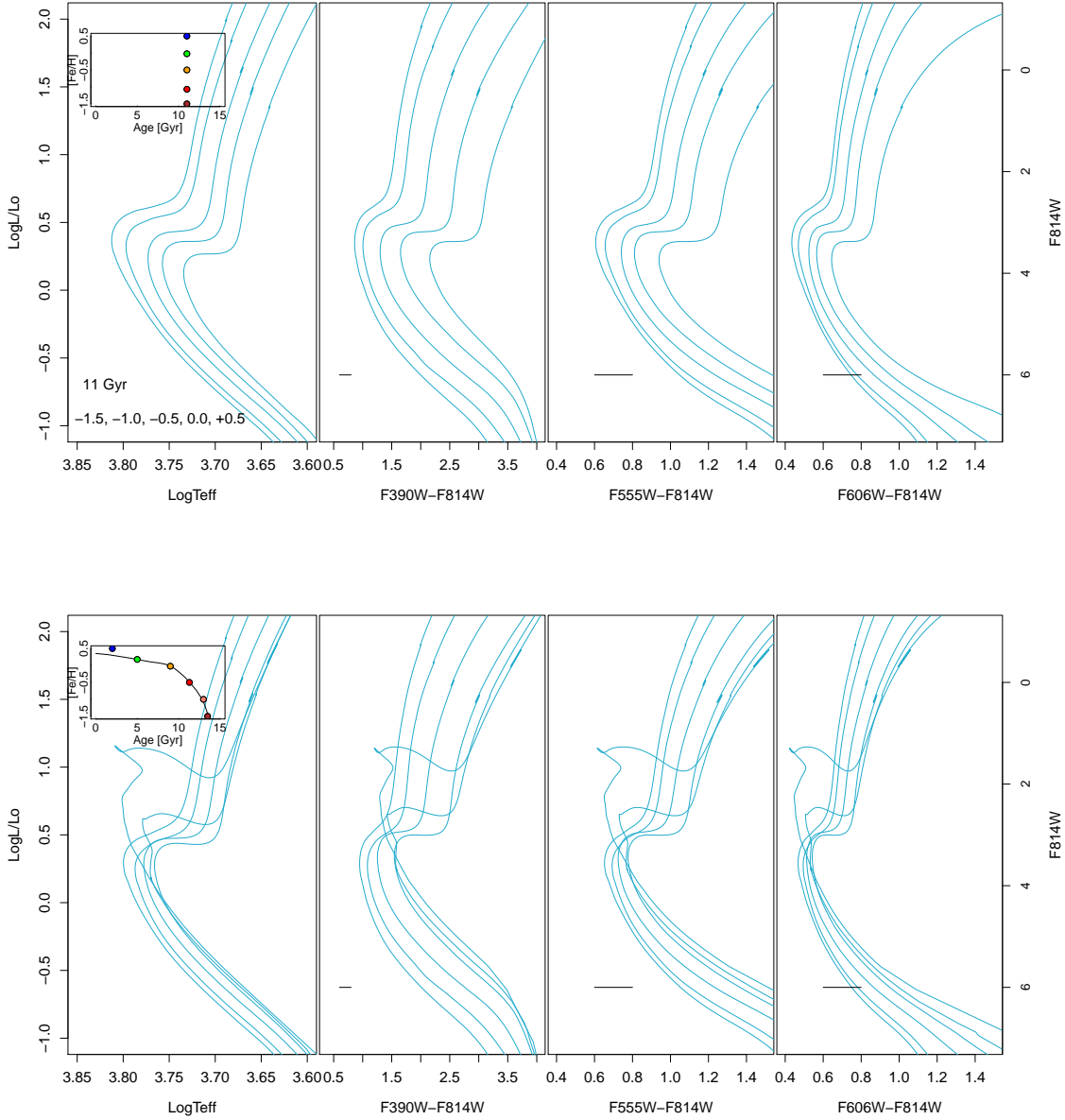


Fig. 7: Isochrones from Dartmouth at age 11 Gyr and metallicities ranging from -1.5 to +0.5 dex (top) and along the age-metallicity relation of Fig. 3 (bottom), in the theoretical CMD in different WFC3 colors. The horizontal short segment in each CMD is 0.2 mag long, to compare with the width of the turn-off in each color band. The color separation at turn-off between the most metal-rich and metal-poor isochrones is 0.21 mag (top) and 0.074 mag (bottom) in the F606W-F814W, similarly to Fig. 5 and 3. The color separation at the turn-off is 0.333 and 0.124 mag in the F555W-F814W bands. Alpha abundances of the isochrones are the same as those used for the isochrones of Fig. 5 and Fig. 3.

is no more than ~ 0.08 magnitude between the isochrones at $[\text{Fe}/\text{H}] = -1.5$ (13.5 Gyr) and $[\text{Fe}/\text{H}] = +0.35$ dex (2 Gyr), respectively the bluest and reddest turn-offs in Fig. 3. Note that, because in case (a) the maximum metallicity considered is +0.35 dex, we also limited the spread in metallicity in case (b) and (c) to the same value. No metallicities higher than 0.35 dex have been taken into account when generating the CMDs below. Although it has no effect on case (a) because stars more metal-rich than +0.35 dex are also young, so they do not increase the spread at the turn-off (see the 2 Gyr isochrone on Fig. 3), this selection under-

estimates the intrinsic spread of case (b) and (c) – by at most a few 0.01 mag – strengthening the conclusions of this study.

Fig. 4 (case b) shows an intermediate case where the bulge is represented by an AMR that goes from $[\text{Fe}/\text{H}] = -1.5$ dex at 13.5 to $[\text{Fe}/\text{H}] = +0.5$ dex at 10 Gyr. It is possible that while being old (>10 Gyr), the bulge would have such an AMR. In this case, the range in color is about two times the previous one, or about 0.17 mag.

Fig. 5 (case c) shows a set of 11 Gyr isochrones with different metallicities (from -1.5 to +0.5). The plot illustrates

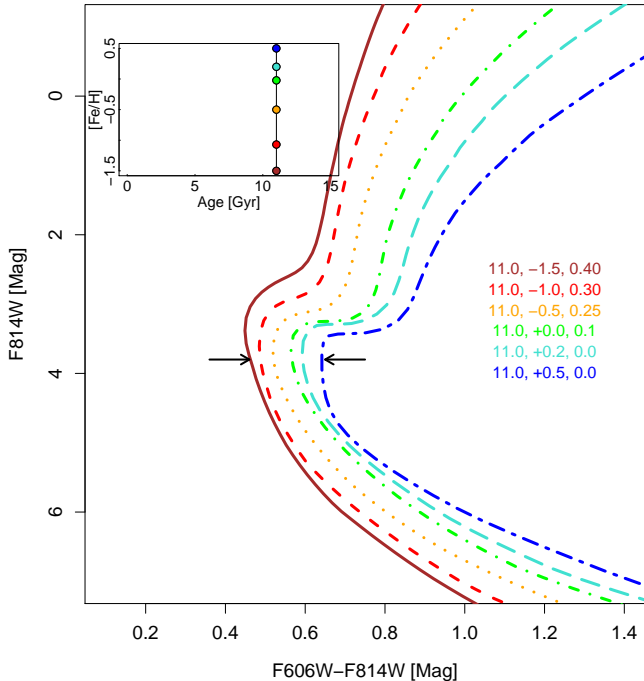


Fig. 5: Case (c): isochrones at age 11 Gyr and metallicities ranging from -1.5 to +0.5 dex. The two arrows at the turn-off are separated by 0.19 mag. The age, metallicity and $[\alpha/\text{Fe}]$ abundance are given for each isochrone.

that a coeval population, having the range of metallicities similar to what is observed for most of the bulge stars, has a wider turn-off (~ 0.2 mag) than the one presented in Fig. 3, as expected. Already from these simple comparisons, it is difficult to figure out how the case for an old, (both with an AMR or coeval) population can be compatible with observations, given that the observed photometric spread is smaller than 0.1 mag at the turn-off, while for case (b) and (c) it is larger than 0.17 mag.

Although a conclusion would be premature, because several other effects have to be taken into account before comparing with the observed CMD (see following section), these results do suggest that given the broad range of metallicities found in the bulge, a uniformly old population (>10 Gyr) would produce a turn-off wider than observed in the studies of CL08, Clarkson et al. (2011) and CA15.

Fig. 6 shows the set of isochrones of case (a) superposed on the CMD data of the SWEEPS field². Isochrones of age 13.5 and 2 Gyr are at the limit of the observed data points but we do not expect much objects at these ages. Between 5 and 13 Gyr, the isochrones are well within the spread observed, and illustrate that case (a) is perfectly possible.

Fig. 7 shows different color plots from other isochrones (Dartmouth database, Dotter et al. 2008) both to confirm the expected spread in color given the metallicity spread ob-

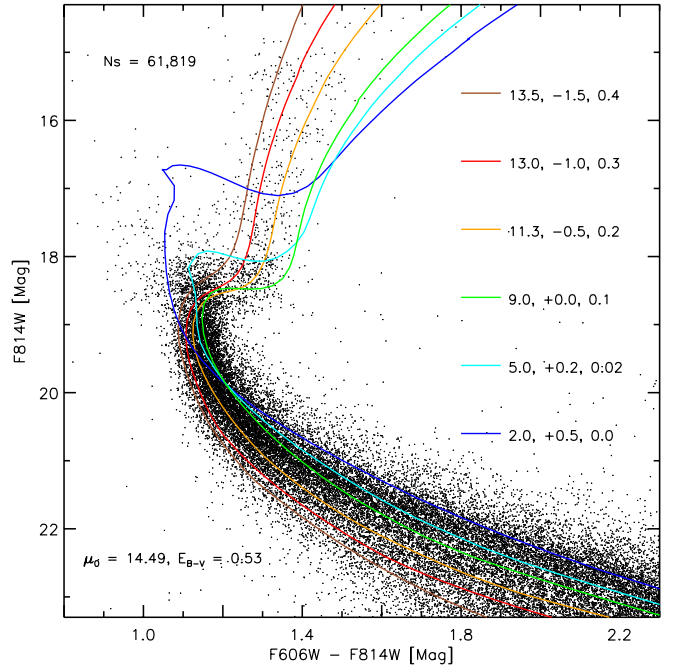


Fig. 6: CMD in the SWEEPS field together with the isochrones of Fig. 3.

served in the bulge using a set of different isochrones, but also to illustrate the expected intrinsic color range at the turn-off using different photometric bands from the HST-WFC3. The combination of F606W and F814W filters is most adapted to study this problem, because this color maximises the difference between the two extreme cases considered here (the case of a uniformly old population of age 11 Gyr and that of a spread of ~ 10 Gyr in age). Hence, although in absolute values the spread at the turn-off is larger in the F390W-F814W filters (1.29 mag compared to 0.21 mag in F606W-F814W for the no-AMR case), the spread is only two times smaller in these filters for the AMR case (from 1.29 to 0.59 mag), when it is three times smaller in F606W-F814W for the AMR case (from 0.21 to 0.074 mag). So the contrast between the cases with and without AMR is expected to be the highest in the F606W-F814W bands.

3.2. Simulated Color-magnitude diagrams and comparison with the observations

We now illustrate this idea further by computing more realistic CMDs for the three cases presented in the previous section, taking into account the depth effect, the differential extinction and binaries through Monte Carlo simulations. Starting from our model distributions, we simulate a set of (age, $[\text{Fe}/\text{H}]$, $[\alpha/\text{Fe}]$) parameters through Monte-Carlo extraction from which we generate isochrones. A position along the isochrone is chosen according to the mass distribution generated from the IMF.

An extraction of ~ 10000 stars is made for each case considered. The 'intrinsic' dispersion (due to age and metallicity effects only, no dispersion due to depth effects, binaries, differential reddening) of each simulation is 0.026 (case a),

² Based on observations made with the NASA/ESA *Hubble Space Telescope*, obtained by the Space Telescope Science Institute. STScI is operated by the Association of Universities for Research in Astronomy, Inc., under NASA contract NAS 5-26555.

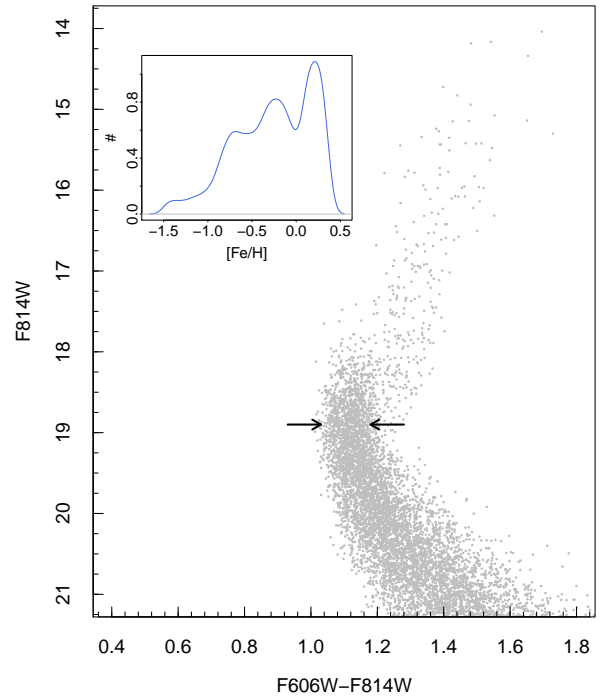
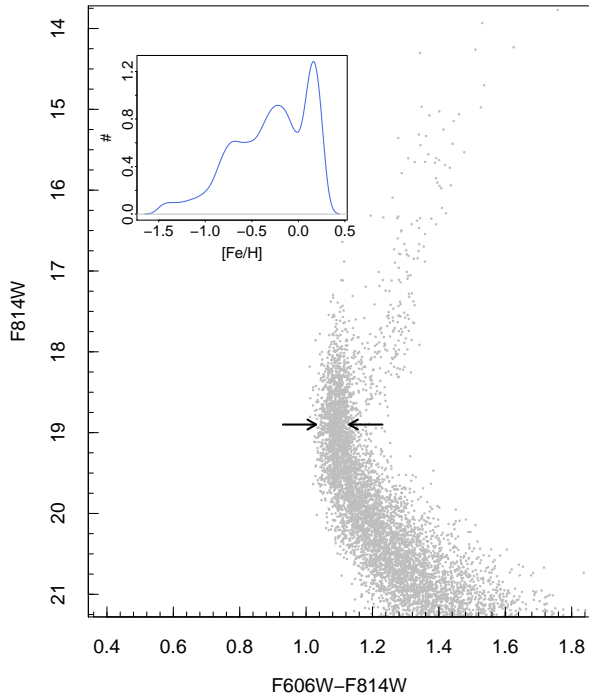


Fig. 8: Monte Carlo simulations of the CMD of Fig. 3 in the F814W/F606W-F814W bands, as described in the text. A dispersion of 0.26 mag has been applied on magnitudes to take into account the spread in distance, 0.016 mag on colors to take the differential extinction into account, and 30% binaries. The two arrows on each plot correspond to separation of 0.10 mag. The inset frame shows the corresponding metallicity distribution of the simulation. The percentage of objects younger than 9 gyr in this plot is 34%.

Fig. 9: Monte Carlo simulations of the CMD of Fig. 4 in the F814W/F606W-F814W bands, assuming the same conditions as in Fig. 8. The two arrows on each plot correspond to separation of 0.15. The inset frame shows the corresponding metallicity distribution of the simulation.

0.036 (b) and 0.044 mag (c). Note that these dispersions decrease to 0.023, 0.032 and 0.041 mag if only metallicities above -1.0 dex are selected, so the tail at low metallicities has a limited effect. From these numbers, it is possible to see that the dispersion obtained for an isochrone population (case c) is hard to reconcile with the observations, being already $\sim 50\%$ larger than the observed dispersion (~ 0.031 mag), given that none of the other sources of dispersion have been taken into account.

In order to obtain more realistic estimates, various contributions must be taken into account. The first one is the depth effect: all stars are not at the same distance, and a variation of ± 1 kpc at 8kpc will translate into a difference in the distance modulus of about $(+0.26, -0.29)$ mag. Following Valenti et al. (2013), a dispersion of 0.26 mag has been added to take into account the spread in distance of stars in the bulge. The dispersion now rises to 0.035, 0.042 and 0.051 ± 0.001 mag, or a spread of 0.105, 0.126 and 0.153 mag.

Another potentially important effect that one has to take into account comes from differential reddening. In CA15, this is taken into account by assuming a possible reddening variation of ± 0.05 mag over the whole field, which we model by assuming a dispersion in reddening of 0.0166 mag. The resulting new dispersions are now 0.039 ± 0.0013 , 0.045 ± 0.0009 and 0.054 ± 0.0012 mag, or a spread of 0.117,

0.135 and 0.162 mag for case (a), (b) and (c) respectively (if metallicities are limited to $[\text{Fe}/\text{H}] > -1.0$ dex, the dispersions are 0.037 ± 0.0010 , 0.043 ± 0.0011 and 0.051 ± 0.0012 mag).

The percentage of binaries and the distribution of their mass ratios is not known for the bulge. We simulate binaries assuming a uniform distribution of mass ratios (Raghavan et al. 2010). Because the Yale stellar track library is limited to stellar masses higher than $0.4 M_{\odot}$, we derived unresolved binary parameters only in cases where the companion has a mass higher than this limit. Because the mass at the turn-off is about $0.8 M_{\odot}$, it implies that companions with an absolute magnitude difference higher than about 4.5 mag are not modelled, corresponding to neglecting effects on combined magnitudes that are smaller than 0.015 mag, which is reasonable. According to CA15, the minimum fraction of binaries is about 30%, but it would easily reach 50% if it was similar to the disk (and if indeed the bulge is essentially made of disk stars). Assuming 30% of binaries, the dispersion increases to 0.051 ± 0.001 mag (case a), 0.056 ± 0.0019 (case b) and 0.064 ± 0.0015 mag (case c). These numbers rise to 0.056 ± 0.0014 , 0.058 ± 0.0017 mag and 0.065 ± 0.0014 in the case of 50% binaries, and 0.056 ± 0.0013 mag (case a) 0.059 ± 0.0014 (case b) and 0.066 ± 0.0015 mag in the case of 100% of binaries. As can be seen, the increase in dispersion is not linear with the fraction of binaries, but varies most rapidly with small percentages, then flattens above 50%.

We conclude that even in case (a) the dispersion is higher than the one measured on the SWEEPS data, which means we have probably overestimated one or several of the sources of dispersion. Even so, it is difficult to imagine that

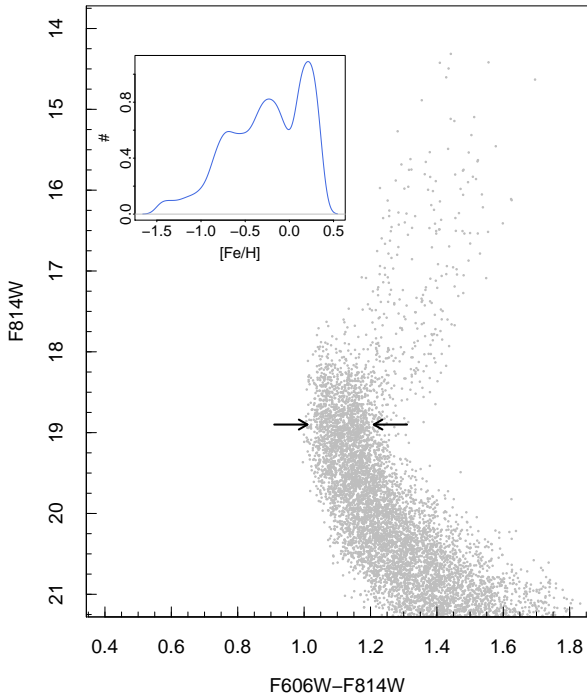


Fig. 10: Monte Carlo simulations of the CMD Fig. 5 in the F814W/F606W-F814W bands, assuming the same conditions as in Fig. 8. The two arrows on each plot correspond to separation of 0.20 mag. The inset frame shows the corresponding metallicity distribution of the simulation.

the dispersion in cases (b) and (c) can be reconciled with a dispersion lower than 0.03 mag as the one observed, being already larger than this limit when only age and metallicity are taken into account. The freedom that we have to accommodate for a smaller dispersion in case (a) is larger because, in addition to the possible overestimated differential reddening, distance uncertainty and effect of binaries, we have not tuned the AMR in any way, nor the SFH, which both play a role in determining the dispersion at the turn-off.

In addition, we also note that the spread in color of the giant branch is also remarkably tight in Clarkson et al. (2011, their Fig. 1), being limited to at most 0.2 mag. This is also in much better agreement with case (a) than with case (c), where it can be seen that the spread is about 0.4 mag.

Hence, the present study proves that the bulge must contain young disk stars in substantial amount if we want the spread of metallicities observed in several independent studies to be compatible with an apparently uniformly old bulge as observed from its CMD. If the bulge contains metal-rich stars, these have to be significantly younger than the subsolar metallicity population.

A final comment is worth making. We find that the CMD is not compatible with a unique (old) age given the spread in the metallicities, but this statement is true at all ages. In other words, the observed CMD is also a constraint on the dispersion of the age-metallicity relation in the inner-disk and bulge, and tells us that this relation must be relatively tight in order to accommodate the spread in

color at the turn-off in the SWEEPS CMD. This is at variance with the age-metallicity relation observed at the solar vicinity for example but in accordance with the closed-box model we assumed for the inner disk and bulge. It tells us that the age-metallicity relation in the inner disk must be tighter, contrary to what is seen in the solar vicinity. Our interpretation is that, the solar vicinity being in the transition region between the inner and outer disk, the metallicity gradient is very steep locally, bringing stars of significantly different metallicities at a given age in the local volume, while in the inner disk the evolution has been much more homogeneous.

4. Discussion

We have shown that:

(1) A coeval stellar population with an age of 11 Gyr and a metallicity distribution compatible with that of the Baade's Window implies a spread in the turn-off color significantly larger than the one observed in the SWEEPS field.

(2) Even for a bulge with an age older than 10 Gyr and in which metallicity correlates with age, the turn-off region should be significantly broader than what is observed in the SWEEPS field.

(3) A bulge population which is assumed to follow the same chemical characteristics (and in particular the same AMR) as those we used to model the inner disk (which is expected if the bulge is a bar formed from the disk) produces a CMD with a tight turn-off, hiding a spread in age of about 10 Gyr, between 3 and 13 Gyr.

These results imply that the presently known constraints from CL08 and Valenti et al. (2013) are not evidence that the bulge is exclusively old (>10 Gyr). On the contrary, they are evidence that the more metal-rich stars in the bulge must be significantly younger than the metal-poor ones, otherwise we would expect the turn-off of the bulge to be significantly broader than observed.

It is worth emphasizing here that we still view the bulge as predominantly old: in our model (see Haywood et al. 2016, in preparation), about 50% of the stars must have ages greater than 9 Gyr. In the CMD of Fig 8, the percentage decreases to 34%, because we considered the SLEEPS field would have a negligible amount of stars younger than 3 Gyr. Clearly, there is room for a younger population, which makes the bulk of the metal-rich peak. This population originate in the inner thin disk (see Di Matteo 2016, for a review), and its stars formed after the quenching episode (Haywood et al. 2016) that occurred at the end of thick disk phase, and so must be essentially younger than 8 Gyr.

Before discussing the evidence from the literature in favor of an exclusively old bulge, it is worth discussing the ages of the metal-rich dwarfs from B13 in the light of our results, and to see in particular how far the age of their metal-rich stars are still compatible, within the error bars, with being old (> 10 Gyr), supposing they are all bulge stars. In their Fig. 4, out of 19 stars having $[\text{Fe}/\text{H}] > 0.1$ dex, 14 have ages compatible with being 5 Gyr old or younger within 1 sigma on $\text{Log}T_{\text{eff}}$ or $\log g$, while only 5 are within one sigma of being 10 Gyr or older. All these 5 stars are also compatible with being younger than 10 Gyr (and for 3 of them, younger than 5 Gyr) within 1 or 2 sigmas. On the contrary, 9 stars younger than 10 Gyr are irreconcilably hotter than the 10 Gyr isochrone, being sometimes off by

more than 500 K (4 to 5 σ on temperature). This is to emphasize the fact that, while all metal-rich stars of B13 are reasonably (within 1 or 2 sigmas) compatible with being young (5 Gyr or younger), the reverse is not true, and no young star in B13 is compatible with being 10 Gyr old or older (within less than 4 to 5 sigmas on $\text{Log}T_{\text{eff}}$), although this would be expected if the bulge was exclusively old. We now review the arguments that have been invoked to support that the metal-rich population must be exclusively old.

(1) The stellar population arguments

Up to the nineties, the Galactic bulge has been essentially associated to an old, collapsed component (e.g. Rich 1990; Matteucci & Brocato 1990) and it has been suggested that even its metal-rich stars could be older than the halo component (Renzini & Greggio 1990). Two results mainly have concurred to support the idea of a uniformly old bulge, even though the possibility of young super metal-rich stars has been recognized early (Wood & Bessell 1983). The first is the prediction by Matteucci & Brocato (1990) that alpha-enhanced abundances were to be expected even at high metallicities, and the first observations supported this prediction (McWilliam & Rich 1994). The second is the idea that the angular momentum distribution of the bulge is similar to the one of the halo – the thick disk having similar distribution to the thin disk – thereby linking the bulge to a primordial collapse of the Galaxy, see e.g. Wyse & Gilmore (1992). While we discuss the chemical argument in more detail below, it is worth emphasizing that subsequent studies have not confirmed the substantially enhanced alpha abundances at solar metallicities and above.

The discovery that the bulge is in fact a bar (Blitz & Spergel 1991), and the discovery that vertical instabilities create boxy and peanut shape morphologies (Combes & Sanders 1981) has prompted the idea that at least part of the bulge could be made of disk stars trapped into the bar, with the dual nature of the bulge already suggested at this time (Rich 1993). However, the measurement of alpha-enhanced abundances at high metallicities (McWilliam & Rich 1994; Lecureur et al. 2007) and the seemingly old CMD (CL08) suggested up to recently that the bulge was a mixture of a classical and pseudo-bulge, prompting the presentation of more sophisticated chemical evolution models with uniformly old bulge, even at high metallicities (Ballero et al. 2007; McWilliam et al. 2008).

It has been argued at the same time from kinematic arguments that if a classical bulge exist in the MW, it must either be small, or inexistent (Shen et al. 2010, Kunder et al. 2012, Di Matteo et al. 2014, Kunder et al. 2016 estimated its mass to be 1% of the total mass of the inner Galaxy). If the classical bulge is small, it implies that the bulge of the MW must be a pseudo-bulge, that is a bulge formed from the disk through dynamical instabilities. The evidence that most of the bulge is a pseudo-bulge is now overwhelming. The last evidence came from the finding by McWilliam & Zoccali (2010) and Nataf et al. (2010) that the bulge is X-shaped. It has been shown in Di Matteo et al. (2014, 2015) how the disk inside the Outer Linblad resonance radius can be mapped into the bar and how the stellar components detected by Ness et al. (2013) can be identified to the thick and thin disks of the MW (Di Matteo 2016), while the peanut-shape is seen to be most prominent in the metal-rich component (Ness et al. 2013), clearly pointing to a disk origin.

This rapid summary shows that within a little more than a decade, new data on the structural shape and kinematical characteristics have changed our view of the bulge, from a collapsed, rapidly formed spheroidal component to a bar formed from dynamical instabilities in the disk. These arguments are not direct evidence that the metal-rich objects must be younger than ages expected for an old spheroid formed by mergers (as often advocated for a classical bulge), but they are evidence of a disk origin of these stars. Because there is no clue that metal-rich stars in the disk must be older than 10 Gyr, it is reasonable to expect those seen in the bulge to be also younger than this limit.

(2) The chemical argument

As mentioned previously, it has been argued that, because the bulge is α -rich compared to the solar vicinity, it formed on a short time scale (e.g. Zoccali et al. 2006; Grieco et al. 2012). While it has been found in the first studies that metal-rich bulge stars seemed to be systematically more alpha-enhanced than local disk stars, the offset has only been decreasing in the last ten years. Most recently, studies made on the same type of stars (dwarfs) by the same group using the same method (B13 and Bensby et al. 2014) obtained results that are almost indistinguishable.

Johnson et al. (2012) argued that the low ratio of [La/Eu] indicates that the majority of the bulge formed rapidly ($<1\text{Gyr}$). Fig. 11 compares the [La/Eu] abundance ratio for two different bulge samples from Johnson et al. (2012) and Van der Swaelmen et al. (2016), together with three different samples of solar vicinity stars from Battistini & Bensby (2016), Mishenina et al. (2013) and Ishigaki et al. (2013). They all show good agreement, and the two bulge samples show no evidence of having lower [La/Eu] than solar vicinity stars. We conclude that the available [La/Eu] abundance ratios do not provide evidence that the bulge formed faster than the inner disk. Other arguments are put in the balance for an old bulge by Nataf (2015), such as the presence of RR Lyrae and old globular clusters. However, these only confirm (if it was needed) that there are old populations in the bulge, but does not imply that the bulge must be exclusively old.

More generally, it is important to emphasize that there is no argument coming from chemical evolution modelling asserting that the metal-rich population must be old. The original results from Matteucci & Brocato (1990) are based on the endorsing a uniformly old age for the bulge (and particularly for metal-rich stars), reflecting a generally accepted idea of that time³. The most recent Galactic Chemical Evolution (GCE) models are still trying to cope with representing the bulge as exclusively old, and the HST CMD of a seemingly old population has a heavy weight in this choice. Although they reproduce reasonably well the observed chemical constraints, we want to emphasize that: (1) these models see the bulge as a component isolated from the disk, which is unrealistic given the present evidence of the bulge being mostly a pseudo-bulge, (2) Modelling the bulge as an exclusively old and isolated system imposes a complexity and a number of adhoc parameters which are actually not required by the data if the bulge is considered

³ This subject was then pretty much in the air, see for example Frogel (1990): 'Whether or not the Galactic bulge contains a detectable population of stars with age much less than 10 Gyr is a subject of considerable debate', to conclude that the bulge has no evidence for a population younger than 10 Gyr.

as a bar grown from the disk and having the age range of the disk. In Grieco et al. (2012), the metal-rich component is modelled with parameters different than those used for stars below $[\text{Fe}/\text{H}] < 0.0$ dex. The infall time scale, star formation efficiency, and IMF are assumed to be different than that of the stars at lower metallicities. In Tsujimoto & Bekki (2012), the metal-rich component is formed from gas at a metallicity $[\text{Fe}/\text{H}] \sim -0.3$ dex, which, having to form stars on a short time scale, also implies a top-heavy IMF. GCE models are able to produce the metal-rich component as being exclusively old, but this comes with a price, because forming stars enriched to $[\text{Fe}/\text{H}] > +0.3$ dex in a limited amount of time (within a few Gyr) is challenging. This is usually done by endorsing a flatter IMF than the one used for the solar vicinity, for instance a Salpeter IMF, or even flatter (Matteucci et al. 1999; Ballero et al. 2007; Tsujimoto & Bekki 2012; Grieco et al. 2012). In this context, it is worth mentioning that CA15 measure an IMF for the bulge population which is compatible with that of the disk, and different from the Salpeter IMF. Also, while it is sometimes recognised in these studies that the (metal-rich) bulge is a bar formed from disk material, these models still represent this component with specific and adhoc parameters which differ from those adopted to reproduce the metal-poor component, but with little justification. For example, in Grieco et al. (2012) metal-rich stars are formed within less than 1 Gyr after the metal-poor population, but no argument justifies that the star formation efficiency is decreased by more than a factor of 10 (from 25 Gyr^{-1} to 2 Gyr^{-1}) in such short amount of time, or that the time scale for infall is increased by a factor of 30 (from 0.1 to 3 Gyr).

5. Conclusions

We conclude this study by saying that there is no evidence from the CMD in the SWEEPS field that the bulge is exclusively old. The HST CMD has been claimed to provide the best evidence of an old bulge, but it is in fact evidence of the contrary: the tight turn-off of the CMD is possible only if it is hiding a correlation between age and metallicity, which means that metal-rich stars ($[\text{Fe}/\text{H}] > 0$) must be significantly younger than the metal-poor population ($[\text{Fe}/\text{H}] < 0$ dex). In Haywood et al. (in preparation), we show that a model which represents the bulge with a thick and a thin disk reproduces well observed chemical constraints, with no additional parameters than those used to represent the thin and thick inner disks. Evidently, since we model the bulge with a thick+thin disk populations, we release the constraint of having ages greater than ~ 10 Gyr only. This makes the production of metal-rich stars much easier, and in particular there is no need to assume an IMF different from that of the disk. In our model, stars having $[\text{Fe}/\text{H}] > 0$ dex are all younger than 8 Gyr, and are formed after the quenching episode (Haywood et al. 2016). Our results show that unless the MDF in the SWEEPS field is strongly different from that of the neighbouring Baade's Window, these younger stars are necessary to reproduce the CMD obtained from the HST.

Acknowledgements. We are grateful to the referee for a detailed report and very helpful comments. A.C. acknowledges NASA which supported her work through grants GO-9750 and GO-12586 from the Space Telescope Science Institute, which is operated by AURA, Inc., under NASA contract NAS 5-26555.

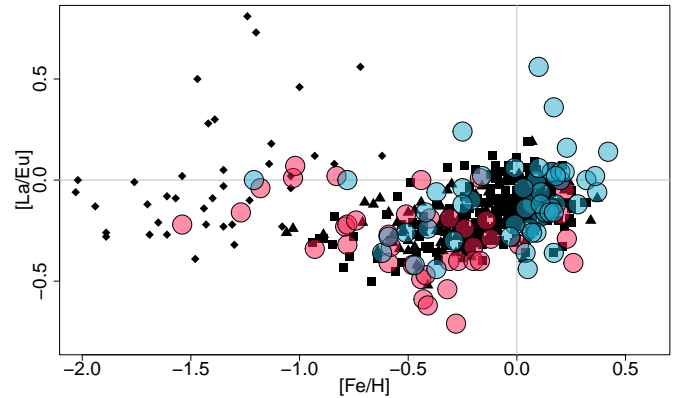


Fig. 11: $[\text{La}/\text{Eu}]$ from Johnson et al. (2012) and Van der Swaelmen et al. (2016) (respectively pink and blue larger symbols) of bulge stars compared to data from Battistini & Bensby (2016) (triangles), Mishenina et al. (2013) (squares) and Ishigaki et al. (2013) (diamonds) for solar vicinity stars. There is no evidence from this data that the bulge and the solar vicinity distributions are different.

References

- Adibekyan, V. Z., Sousa, S. G., Santos, N. C., et al. 2012, *A&A*, 545, A32
- Ballero, S. K., Matteucci, F., Origlia, L., & Rich, R. M. 2007, *A&A*, 467, 123
- Battistini, C., & Bensby, T. 2016, *A&A*, 586, A49
- Bedin, L. R., Cassisi, S., Castelli, F., et al. 2005, *MNRAS*, 357, 1038
- Bensby, T., Adén, D., Meléndez, J., et al. 2011, *A&A*, 533, A134
- Bensby, T., Yee, J. C., Feltzing, S., et al. 2013, *A&A*, 549, A147
- Bensby, T., Feltzing, S., & Oey, M. S. 2014, *A&A*, 562, A71
- Blitz, L., & Spergel, D. N. 1991, *ApJ*, 379, 631
- Calamida, A., Sahu, K. C., Anderson, J., et al. 2014, *ApJ*, 790, 164
- Calamida, A., Sahu, K. C., Casertano, S., et al. 2015, *ApJ*, 810, 8
- Clarkson, W., Sahu, K., Anderson, J., et al. 2008, *ApJ*, 684, 1110
- Clarkson, W. I., Sahu, K. C., Anderson, J., et al. 2011, *ApJ*, 735, 37
- Combes, F., & Sanders, R. H. 1981, *A&A*, 96, 164
- Demarque, P., Woo, J.-H., Kim, Y.-C., & Yi, S. K. 2004, *ApJS*, 155, 667
- Di Matteo, P., Haywood, M., Gómez, A., et al. 2014, *A&A*, 567, AA122
- Di Matteo, P., Gómez, A., Haywood, M., et al. 2015, *A&A*, 577, A1
- Di Matteo, P. 2016, arXiv:1603.05485
- Dotter, A., Chaboyer, B., Jevremović, D., et al. 2008, *ApJS*, 178, 89-101
- Erwin, P., Saglia, R. P., Fabricius, M., et al. 2015, *MNRAS*, 446, 4039
- Fisher, D. B., & Drory, N. 2010, *ApJ*, 716, 942
- Fisher, D. B., & Drory, N. 2016, *Galactic Bulges*, 418, 41
- Frogel, J. A. 1990, *European Southern Observatory Conference and Workshop Proceedings*, 35, 177
- Fulbright, J. P., McWilliam, A., & Rich, R. M. 2007, *ApJ*, 661, 1152
- Gonzalez, O. A., Rejkuba, M., Zoccali, M., et al. 2011, *A&A*, 530, A54
- Gonzalez, O. A., Zoccali, M., Vazquez, S., et al. 2015, *A&A*, 584, A46
- Grieco, V., Matteucci, F., Pipino, A., & Cescutti, G. 2012, *A&A*, 548, A60
- Haywood, M., Di Matteo, P., Lehnert, M. D., Katz, D., & Gómez, A. 2013, *A&A*, 560, A109
- Haywood, M., Di Matteo, P., Snaith, O., & Lehnert, M. D. 2015, *A&A*, 579, A5
- Haywood, M., Lehnert, M. D., Di Matteo, P., et al. 2016, *A&A*, 589, A66
- Hill, V., Lecureur, A., Gómez, A., et al. 2011, *A&A*, 534, A80
- Ishigaki, M. N., Aoki, W., & Chiba, M. 2013, *ApJ*, 771, 67
- Iwamoto, K., Brachwitz, F., Nomoto, K., et al. 1999, *ApJS*, 125, 439
- Johnson, C. I., Rich, R. M., Kobayashi, C., & Fulbright, J. P. 2012, *ApJ*, 749, 175
- Johnson, C. I., Rich, R. M., Kobayashi, C., Kunder, A., & Koch, A. 2014, *AJ*, 148, 67

- Karakas, A. I. 2010, MNRAS, 403, 1413
- Kormendy, J., Drory, N., Bender, R., & Cornell, M. E. 2010, ApJ, 723, 54
- Kormendy, J., & Kennicutt, R. C., Jr. 2004, ARA&A, 42, 603
- Kroupa, P. 2001, MNRAS, 322, 231
- Kunder, A., Koch, A., Rich, R. M., et al. 2012, AJ, 143, 57
- Kunder, A., Rich, R. M., Koch, A., et al. 2016, ApJ, 821, L25
- Lecureur, A., Hill, V., Zoccali, M., et al. 2007, A&A, 465, 799
- Matteucci, F., & Brocato, E. 1990, ApJ, 365, 539
- Matteucci, F., Romano, D., & Molaro, P. 1999, A&A, 341, 458
- McWilliam, A., & Rich, R. M. 1994, ApJS, 91, 749
- McWilliam, A., Matteucci, F., Ballero, S., et al. 2008, AJ, 136, 367
- McWilliam, A., & Zoccali, M. 2010, ApJ, 724, 1491
- Mishenina, T. V., Pignatari, M., Korotin, S. A., et al. 2013, A&A, 552, A128
- Nataf, D. M., Udalski, A., Gould, A., Fouqué, P., & Stanek, K. Z. 2010, ApJ, 721, L28
- Nataf, D. M. 2015, arXiv:1509.00023
- Ness, M., Freeman, K., Athanassoula, E., et al. 2013, MNRAS, 430, 836
- Nomoto, K., Tominaga, N., Umeda, H., Kobayashi, C., & Maeda, K. 2006, Nuclear Physics A, 777, 424
- Raghavan, D., McAlister, H. A., Henry, T. J., et al. 2010, ApJS, 190, 1
- Raiteri, C. M., Villata, M., & Navarro, J. F. 1996, A&A, 315, 105
- Renzini, A., & Greggio, L. 1990, European Southern Observatory Conference and Workshop Proceedings, 35, 47
- Rich, R. M. 1990, ApJ, 362, 604
- Rich, R. M. 1993, Galaxy Evolution. The Milky Way Perspective, 49, 65
- Rojas-Arriagada, A., Recio-Blanco, A., Hill, V., et al. 2014, A&A, 569, A103
- Ryde, N., & Schultheis, M. 2015, A&A, 573, A14
- Shen, J., Rich, R. M., Kormendy, J., et al. 2010, ApJ, 720, L72
- Snaith, O. N., Haywood, M., Di Matteo, P., et al. 2014a, ApJL, 781, L31
- Snaith, O., Haywood, M., Di Matteo, P., et al. 2015, A&A, 578, A87
- Tsujimoto, T., & Bekki, K. 2012, ApJ, 747, 125
- Valenti, E., Zoccali, M., Renzini, A., et al. 2013, A&A, 559, A98
- Van der Swaelmen, M., Barbuy, B., Hill, V., et al. 2016, A&A, 586, A1
- Wood, P. R., & Bessell, M. S. 1983, ApJ, 265, 748
- Wyse, R. F. G., & Gilmore, G. 1992, AJ, 104, 144
- Zoccali, M., Lecureur, A., Barbuy, B., et al. 2006, A&A, 457, L1